

Neutron Transmission Spectroscopic Imaging for Analysis of Texture in Materials for Industrial Use

Y. Kiyanagi¹, H. Sato¹, O. Takada¹, N. Ayukawa¹, T. Kamiyama¹

¹ Graduate School of Engineering, Hokkaido University, Sapporo, Japan

Email contact of main author: Kiyanagi@qe.eng.hokudai.ac.jp

Abstract. The total neutron cross section has special features reflecting the crystal structure for the coherent scattering material and also the dynamics in the material for the incoherent scattering material. An image indicating the number density, the crystal structure, the preferred orientation, and the strain of the material can be obtained by using the time-of-flight energy analysis coupled with a two-dimensional position sensitive detector at a pulsed neutron source. Here, first the principle of spectroscopic imaging using the time-of-flight method at a pulsed neutron source is described and the images including the information written above are described for an unbended iron plate and a Pb-Bi eutectic. It is suggested that the spectroscopic imaging has ability to evaluate quantitatively the texture information of the materials and to inspect the complex phase change in the materials.

1. Introduction

Neutron diffraction is usually used for non-destructive inspection of material structures and has played an important role in determination of residual strain in engineering applications such as vehicle engines, railway wheels, welding ducts, and others, since the penetration power of neutron is much higher than X-ray[1-3]. Non-destructive material analysis giving an imaging including information on the crystal structure and the texture is very useful to assess the materials for industrial use while the neutron scattering experiments usually give the information of the very small area, for example 2 mm². The neutron radiography is widely used to inspect the inside of the objects, which measurements are performed usually at steady neutron sources such as reactors. The contrast of the image is due to transmission relating to the total cross section over wide energy range. However, the neutron cross section has special energy dependent features since the neutron cross section is expressed by a function reflecting the structure and the dynamics of the materials. The total neutron cross section includes all contribution of the neutron scattering effect and the capture. The scattering consists of the coherent and the incoherent scattering cross sections. The coherent cross section is major component in almost all elements. A very important exception is light-hydrogen. Differences in the structure of the total cross section mainly appear at low energy region, namely cold neutron region. The Bragg edges are observed at the longest wavelength corresponding to 90 degrees of the Bragg's law. The wavelength of the Bragg edge relates to the lattice constant, and the shape the preferred orientation.

Neutron transmission using a pulsed neutron source coupled with a two-dimensional position sensitive detector can give the total neutron cross section of the material corresponding to the each pixel of the detector. By analyzing such data we can get the information on the crystal structure, the strain, the number density, the preferred orientation, the crystallite size, phase transition and so on[4-12]. The phase transition is also observed by watching the Bragg edge change of stainless steel. There are many kinds of patterns of the Bragg edge changes, and now it is difficult to predict such changes theoretically. Therefore, it is important at this stage to examine the various kinds of changes of the Bragg edge patterns in order to clarify the reason of the change and the quantitative estimation of the texture information.

Here, we first present the position dependence of phase transition in Pb-Bi eutectic (LBE) that is a candidate for a target of the accelerator driven system and also for the coolant of the fast

reactor. This material has a problem of expansion after solidification that may cause rupture of the circulating pipe. Second, the preferred orientation and the strain are investigated for a sample of an unbended iron plate in order to know the change of the texture and the lattice parameter. Finally, the effect of the crystallite size is also studied by using the different grain size SS plate, since the reason of the reduction of the cross section around the Bragg edge may be attributed to the grain size.

2. Principle of Spectroscopic Imaging Using a Pulsed Neutron Source

2.1. Total Neutron Cross Section

For the spectroscopic imaging it is firstly required to obtain the energy dependent total neutron cross section on each pixel of the two-dimensional position sensitive detector (2D-PSD). An example of the total neutron cross section of Mo is shown in *FIG. 1* as a coherent scattering case. Many of materials, not only single element but also alloys, have similar structure. At high energy region the resonance peaks appear. After then, a region having no remarkable structure continues to the low energy region. At low energy region many Bragg edges appear. The edge correspond to the Bragg's law, $\lambda=2d_{hkl}$, since the Bragg angle is 90 degrees. Here, λ is the neutron wavelength and d_{hkl} is the lattice spacing of (hkl) lattice plane. At the higher energy region after the edges, the cross section decreases as shown in *FIG. 1*. However, this is not all the case, since the shape depends on the preferred orientation of the crystallite. The shape becomes round if the distribution of the crystallite is anisotropic. After the lowest energy where the Bragg scattering occurs, the cross section falls down suddenly and then gradually increases with decreasing energy due to absorption and inelastic scattering. However, in this region no structure appears.

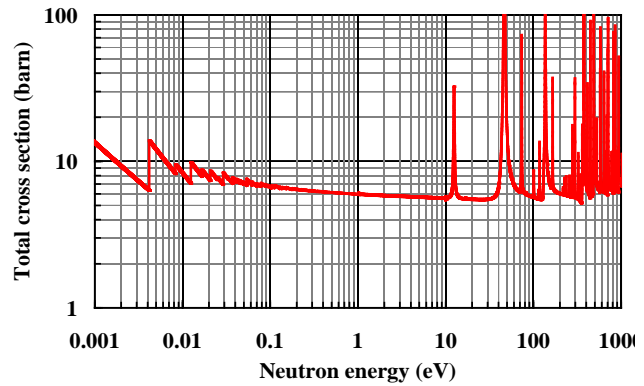


FIG. 1 Example of structure of total neutron cross section.

2.2. Measurement of Spatial Dependent Total Neutron Cross Section

In the pulsed neutron imaging using the time of flight (TOF) method, we observe the incident neutron TOF spectra and the transmitted neutron TOF spectra as shown in *FIG. 2*. The distortion of the incident spectrum is clearly observed in the transmitted spectrum due to the Bragg scattering. A 2D-PSD is used to get the spatial dependent TOF data. The macroscopic total neutron cross section, Σ , is calculated by a formula shown below.

$$\Sigma_{tot}(\lambda) = -\frac{\ln\left(\frac{I(\lambda)}{I_0(\lambda)}\right)}{b}$$

Here, $I(\lambda)$ is the transmitted neutron wavelength spectra, $I_0(\lambda)$ the incident one, and b the thickness of the object. The total cross section is obtained at each pixel. By analyzing the cross section and choosing the data corresponding to items interested in, we can obtain an image concerning to the item.

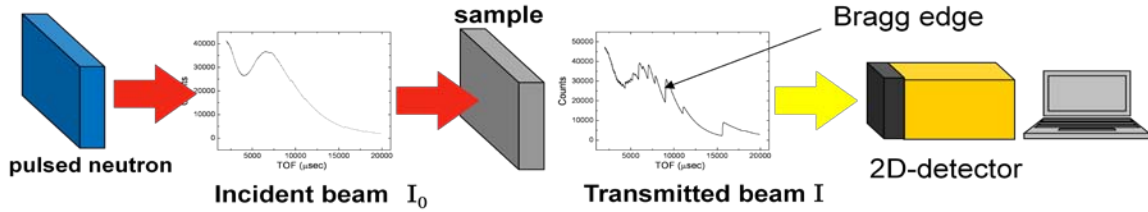


FIG. 2 Schematic experimental setup for spectroscopic imaging at a pulsed source.

2.3. Information Obtained by Spectroscopic Imaging

As recognized easily, an image of element distribution is obtained by the resonance peak assignment since the energies of the resonance peaks correspond to the specific elements. The width of the resonance peak gives information on the temperature as known as Doppler effects in the reactor physics. The temperature distribution measurement is one of the major applications of this method. However, in this paper we do not deal with this item.

The position of the Bragg edge gives information of the crystal structure of the object. So, the phase transition can be easily observed. Furthermore, the wavelength is precisely determined by the time-of-flight measurement with high time resolution. The strain defined by $\varepsilon = (d - d_0)/d_0$, where d_0 is lattice spacing without strain and d is observed one, is obtained and the image of the strain is also presented. The preferred orientation affects the shape of the Bragg edge region, so by analyzing the shape we can obtain the preferred orientation. For analyzing the transmission data we have prepared the data analysis code[13], which is capable of deducing lattice spacing, preferred orientation and number density. For estimating the preferred orientation, March-Dollase function was used[14-15].

3. Experimental methods

We performed the experiments at Hokkaido electron linac facility and at BL10 beam line at Japan Spallation Neutron Source at J-PARC. The power of J-PARC was about 100 times higher than that of Hokkaido linac at that time when the experiments performed. However, the J-PARC power will increase 300 times more. Here, we explain the experimental setups used at both facilities.

3.1. Hokkaido Electron Linac Facility

The neutron source at Hokkaido linac is a solid-methane coupled moderator to obtain higher intensity compared with a decoupled moderator. So, the pulse width of the emitted neutrons is relatively wide. The power of the linac was about 1 kW. The experimental setup is indicated in FIG. 3.

The distance from the moderator to the sample was about 7m. As a 2D-PSD a pixel-type Li-glass detector was used[16]. A photo of the detector is shown in FIG. 4. The detector consists of $16 \times 16 = 256$ Li-glass pixels. Each pixel directly connects to 256 channel photo-multiplier to

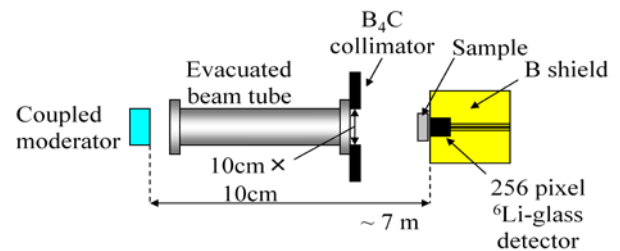


FIG. 3 Experimental setup at Hokkaido linac.

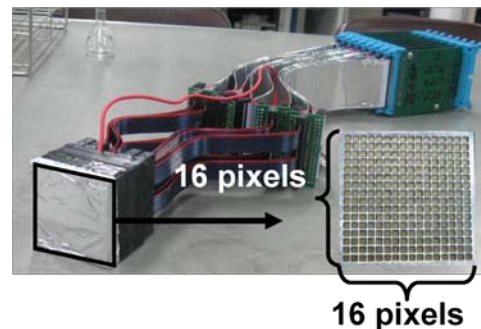


FIG. 4 Photo of 16x16 pixel detector.

obtain a high counting rate. The detection efficiency at the cold neutron region is more than 95% and the counting rate is more than 200MHz per pixel. The pixel size is 3mm square.

3.2. BL10 Beam Line at J-PARC Neutron Source

Neutron experiments are performed in Material Life Science Experimental Facility (MLF) at J-PARC[17]. There are 23 beam lines in the experimental hall. The experimental setup at BL10 at J-PARC is indicated in FIG. 5. The BL10 beam line is used for various kinds of test experiments. Imaging at J-PARC is now under a developing phase. The flight path length is about 14 m. The

moderator is a decoupled para-hydrogen moderator, which has relatively narrow neutron pulse[17]. The power of accelerator was 3 kW at that time. There

are two collimators in the beam line, the sizes were 8.49 cm square, and 7.29 cm square, and the pixel type detector was used. The cold neutron intensity is about 50 times higher than that of Hokkaido linac. A long flight path and narrow neutron pulse enabled us to perform high resolution measurements.

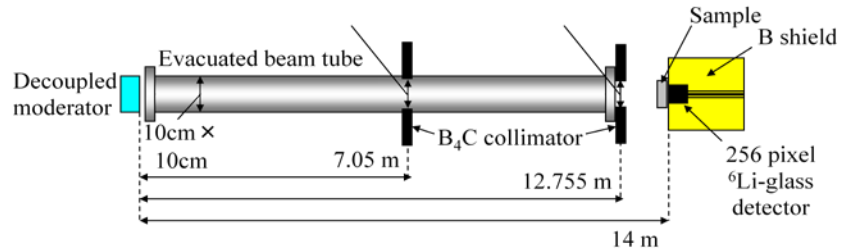


FIG. 5 Experimental setup at BL10 at MLF, J-PARC.

4. Applications of Spectroscopic Imaging Using a Pulsed Neutron Source

LBE structural change, crystal structure image of an unbended iron and an effect of grain size to the total cross section have been studied as application examples of this method.

4.1. LBE structure change with time and position

LBE is a candidate for spallation target and a coolant of Accelerator Driven System since LBE has low slowing down power for neutrons and low melting temperature. However, LBE expands after solidification, which may cause rupture of coolant tube if liquid LBE is solidified accidentally. Solid LBE has two solid phases, β -phase (intermetallic compound) and γ -phase (solid solution Pb in Bi). β -phase is hcp structure and γ -phase is rhombohedral structure. Expansion results from phase transformation β to γ , since rhombohedral structure of γ -phase occupies more space than hcp structure. The reason of the expansion was studied by X-ray diffraction [18], and showed that growth of γ -phase related to the expansion. However, X-ray can see only the surface of LBE. Therefore, we studied the phase transformation in LBE with neutrons to see the inside of LBE depending on position and time for a slow cooling LBE sample and a rapid cooling one.

Two types of LBE samples were prepared by different cooling methods[19]. One is rapid cooling (water cooling) LBE and the other slow cooling (cooling in the furnace) one. The change of the total cross section depending on time is shown in FIG. 6 for a rapid cooling LBE. The peaks of γ -phase are $\gamma(110)=0.455\text{nm}$, $\gamma(104)=0.474\text{nm}$ and $\gamma(012)=0.656\text{nm}$. It is recognized that the cross sections of these peaks increase with time, especially for the 0.656nm peak. This data support the results indicated by X-ray data, which suggests the change occurs in whole volume of LBE. Having 8 month period since our preparation we performed experiments on the LBE samples at MLF at J-PARC. The cross section data for two kind samples are presented in FIG. 7. The γ -phase peaks are clearly seen due to high time resolution, namely high wavelength resolution, of the experiments. The statistics are relatively high, so we can make image indicating cross section of $\gamma(012)$. FIG. 8 shows the results for both samples. From these images it is known that the slow cooling sample has

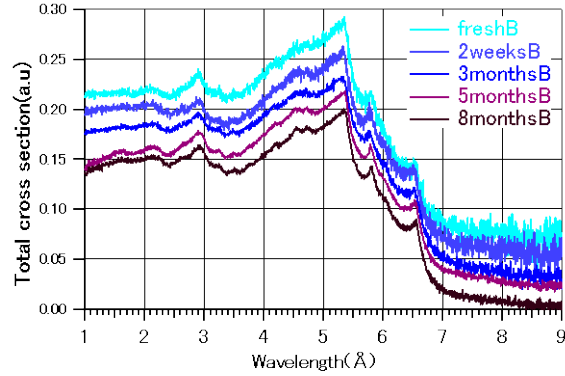


FIG. 6 Time dependent change of total cross sections of a rapid cooling sample obtained by averaging over all used pixels.

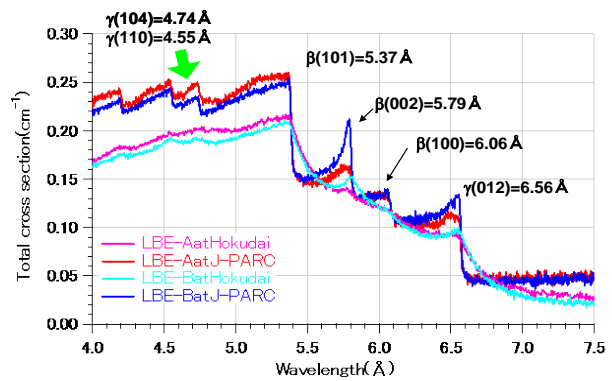


FIG. 7 Total cross sections calculated from J-PARC data. As a reference cross sections obtained at Hokkaido linac are presented, too. LBE-A is the slow cooling and LBE-B the rapid cooling one.

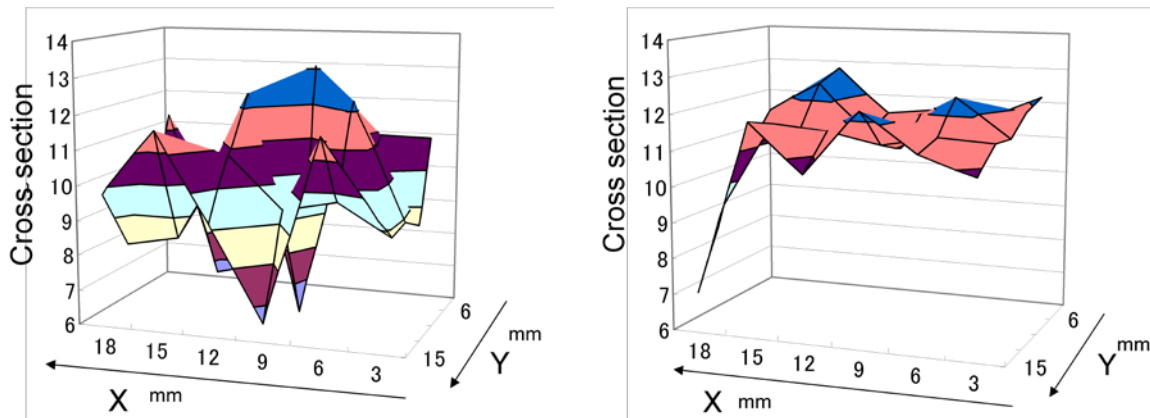


FIG. 8 Distributions of total cross sections of $\gamma(012)$. Left figure is for a slow cooling LBE and right for a rapid cooling LBE.

inhomogeneous distribution of the crystal structure. On the other hand, the structure of the rapid cooling sample is homogeneous. The values of the rapid cooling LBE are higher than those of the slow cooling one, which indicates that the rapid cooling LBE expands faster than the slow cooling one.

4.2. Texture Change of Unbended Iron Plate

We interested in the structure/texture change around highly stressed area. So, we prepared an iron sample that had been bended at two positions and then unbended. The thickness of iron was 5 mm. The transmission data were obtained at MLF. We obtained the data of surface density, preferred orientation and strain by using the data analyzing code. FIG. 9 shows the surface density (density x thickness). Two bended positions apparently recognized as lowest

density positions. The preferred orientation is mapped in FIG. 10. It is indicated that the texture was affected by bending and the higher angle of preferred orientation is observed. The lattice spacing for (110) plane is shown in FIG. 11 and there is about 0.1% difference of the lattice spacing.

4.3. Crystal Size Effect on Total Cross Section

We observed a decrease of total cross section of a heat treated SS compared with untreated one. We speculated that this would be due to the extinction effect of the neutron scattering in the large crystallite, since it is well known that heat treatment makes the grain size larger. To confirm this effect we performed the experiment on the SS samples with different grain sizes. The prepared samples have grain size of 260 and 1190 μm . The total cross section of both sample are indicated in FIG. 12. In this case the cross section of the large grain sample is smaller than the small grain sample. This result supports our speculation, and suggests that we can deduce the size information if we can make simulation code for extinction. Our tentative analysis gave much larger grain size. Therefore, we need more detailed information on grain which may be obtained by other neutron scattering experiment such as small angle neutron scattering.

5. Summary

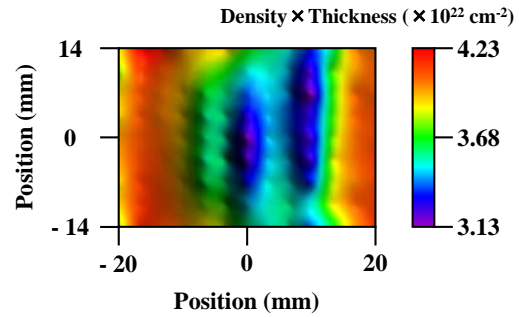


FIG. 9 Surface density distribution.

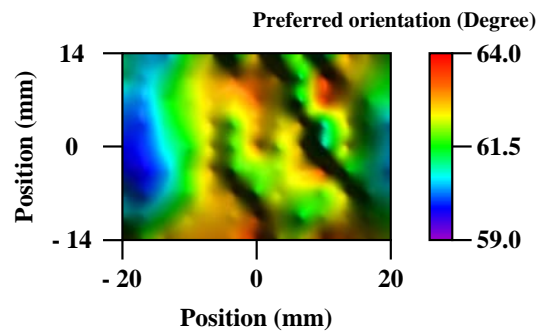


FIG. 10 Distribution of preferred orientation.

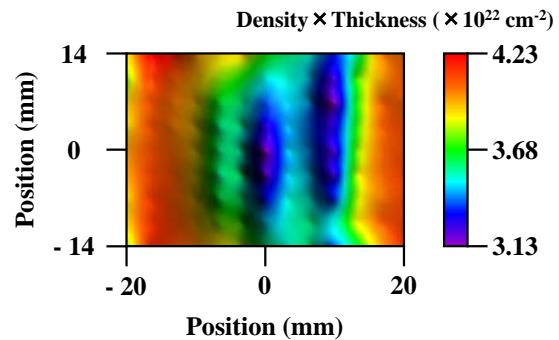


FIG. 11 Distribution of lattice spacing.

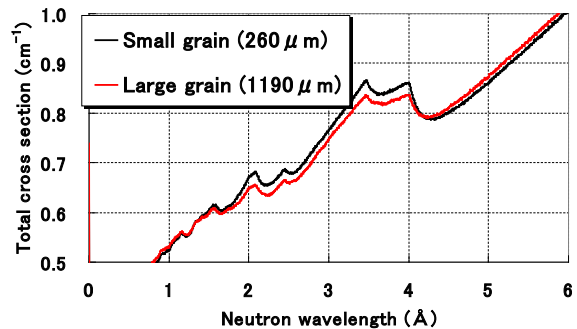


FIG. 12 Change of total cross section due to grain size.

We are developing the spectroscopic imaging by using pulsed neutron sources. It is expected that the information on material texture obtained by this method is very useful for the material characterization and also for the material manufacturing process. However, to obtain quantitative data a simulation calculation code that includes all processes of the neutron scattering in the materials is required and also it is very important to obtain various experimental data indicating many aspects of the total cross section change.

Acknowledgement

The work was supported by a Grant-in-Aid for Creative Scientific Research (No. 20246136) from the Ministry of Education, Culture, Sports, Science and Technology of Japan.

References

- [1] S. Sampath, X.Y. Jiang, J. Matejicek, L. Prchlik, A. Kulkarni, A. Vaidya, *Mater. Sci. Eng. A* 364, (2005) 216.
- [2] M. Grosse, P. Ottliger, *Mater. Sci. Eng. A* 437, (2006) 88.
- [3] S.V. Peace, V. M. Linton, *Physica B* 385-386, (2006) 590.
- [4] J. R. Santisteban, L. Edwards, A. Steuwer and P. J. Withers, *J. Appl. Cryst.* 34, (2001) 289.
- [5] J. R. Santisteban, L. Edwards, M. E. Fitzpatrick, A. Steuwer, P. J. Withers, *Appl. Phys. A* 74, (2002) S1433.
- [6] Y. Kiyonagi, T. Kamiyama, H. Iwasa, F. Hiraga, *Key Engineering Materials* 270 (2004) 1371.
- [7] Y. Kiyonagi, K. Mizukami, T. Kamiyama, F. Hiraga, H. Iwasa, *Nucl. Instr. and Meth. A* 542, (2005) 316.
- [8] Y. Kiyonagi, T. Kamiyama, T. Nagata, F. Hiraga, S. Suzuki, *Physica B* 385 (2006) 930.
- [9] Y. Kiyonagi, T. Kamiyama, O. Takada, K. Morita, K. Iwase, S. Suzuki, M. Furusaka, F. Hiraga, S. Tomioka, K. Mishima, N. Takenaka, T. Ino, *Nucl. Instr. and Meth. A* 600 (2009) 167.
- [10] K. Iwase, K. Sakuma, T. Kamiyama, Y. Kiyonagi, *Nucl. Instr. and Meth. A*, in press.
- [11] H. Sato, T. Kamiyama, Y. Kiyonagi, *Nucl. Instr. and Meth. A*, in press.
- [12] M. A. M Bourke, J. G. Maldonado, D. Masters, K. Meggers, H. G. Priesmeyer, *Mater. Sci. Eng. A* 221, (1996) 1.
- [13] H. Sato, O. Takada, K. Iwase, T. Kamiyama, Y. Kiyonagi, *Proc. International Conference on Neutron Scattering, Noxvill* (2009), to be published.
- [14] K. Mizukami, S. Sato, H. Sagehashi, S. Ohnuma, M. Ooi, H. Iwasa, F. Hiraga, T. Kamiyama, Y. Kiyonagi, *Nucl. Instr. and Meth. A* 529 (2004) 310.
- [15] W.A. Dollase, *J. Appl. Cryst.* 19 (1986) 267.
- [16] S. Vogel, Ph. D. Thesis, Kiel University (2000).
- [17] <http://j-parc.jp/MatLife/ja/index.html>
- [18] H. Grasbrenner, F. Gröschel, H. Grimmer, J. Patorski, and M. Rohde, *Journal of Nuclear Materials*, 343 (2005) 341.
- [19] O. Takada, T. Kamiyama, Y. Kiyonagi, *Proc. International Workshop on Spallation Materials Technology, Sapporo* (2008), to be published.